

## BRIEF COMMUNICATIONS

The purpose of this Brief Communications section is to present important research results of more limited scope than regular articles. Submission of material of a peripheral or cursory nature is strongly discouraged. Brief Communications cannot exceed three printed pages in length, including space allowed for title, figures, tables, references, and an abstract limited to about 100 words.

### Melting and freezing at constant speed

Joseph B. Keller

Departments of Mathematics and Mechanical Engineering, Stanford University, Stanford, California 94305

(Received 21 February 1986; accepted 12 March 1986)

A solution of a one-dimensional melting or freezing problem (i.e., Stefan problem) is found in which the front moves at constant speed.

Suppose that a solid in the region  $x > 0$  is at its melting temperature  $T = 0$  at time  $t = 0$ , and that it is heated at its surface  $x = 0$ . Then a melting front  $x = s(t)$  will move into the solid. We have found that the front moves with constant speed when the applied temperature is given by (3a) or the applied heat flux is given by the exponential function (3b).

To show this we note that the temperature  $T(x, t)$  in the melted region satisfies the following conditions:

$$T_t = DT_{xx}, \quad 0 < x < s(t), \quad t > 0, \quad s(0) = 0, \quad (1)$$

$$T[s(t), t] = 0, \quad -DT_x[s(t), t] = Ls_t. \quad (2)$$

At  $x = 0$  we specify either the temperature to have the value

$$T(0, t) = L(e^{k^2Dt} - 1), \quad (3a)$$

or the heat flux to be given by

$$-DT_x(0, t) = DkLe^{k^2Dt}. \quad (3b)$$

The solution of either problem is

$$T(x, t) = L(e^{k^2Dt - kx} - 1), \quad (4)$$

$$s(t) = kDt. \quad (5)$$

Thus the melting front moves at the constant speed  $kD$ .

If  $L$  is changed to  $-L$  the solution represents a freezing front moving into a liquid at its freezing temperature.

#### ACKNOWLEDGMENT

This research was supported by the Office of Naval Research, the Air Force Office of Scientific Research, the Army Research Office, and the National Science Foundation.

### Energy decay of three-dimensional isotropic turbulence

Iwao Hosokawa

Department of Mechanical Engineering, Iwate University, Morioka 020, Japan

Kiyoshi Yamamoto

National Aerospace Laboratory, Chofu, Tokyo, Japan

(Received 6 December 1985; accepted 10 March 1986)

The trend of energy decay of three-dimensional isotropic turbulence with a particular initial condition for various Reynolds numbers is investigated by comparing the data obtained using different methods. The question is then raised whether the curves of energy decay for different Reynolds numbers can cross each other.

While the energy decay of Burgers' model turbulence has been thoroughly investigated by several authors,<sup>1</sup> that of three-dimensional isotropic turbulence is not yet fully understood. The work on this problem by Kraichnan<sup>2</sup> based on his direct interaction approximation (DIA) theory is probably the earliest. The first direct numerical simulation was performed by Orszag and Patterson, but unfortunately no description of energy decay is found in their publications.<sup>3</sup> Tatsumi, Kida, and Mizushima<sup>4</sup> discussed the energy decay of isotropic turbulence for a wide range of Reynolds numbers on the basis of their modified zero fourth-order

cumulant approximation theory. Their conclusion seems to be, at least qualitatively, persuasive; it predicts reasonable values of the index in the power law of energy decay for high Reynolds numbers, depending on initial conditions. Recently, McComb and Shanmugasundaram<sup>5</sup> calculated energy decay for a relatively low Reynolds number, based on their local energy transfer (LET) theory as well as on the DIA theory, and concluded that the results of both theories are pretty close to each other. It is then interesting to compare the data of energy decay by Tatsumi *et al.* with that of McComb *et al.* in the same figure, but only if the initial con-

dition is common and if the units of energy and time are properly adjusted.

We also performed a direct numerical simulation in essentially the same manner as Orszag *et al.*,<sup>3</sup> in order to pursue the feature of energy decay that is significant for quantitative comparison with other approximation theories. Our initial energy spectrum of isotropic turbulence is taken as

$$E(k) = Ak^4 \exp(-2k^2), \quad (1)$$

where  $k$  is the magnitude of wavenumber and  $A$  is the normalization constant, such that it gives

$$\int_0^\infty E(k)dk = \frac{1}{2}. \quad (2)$$

If the unit of velocity is taken as the root mean (vectorial) square of the initial velocity field and the unit of length as the inverse of the wavenumber with the maximum of the energy spectrum, which is  $k = 1$ , then the Reynolds number  $R_0$  based on these units conveniently becomes  $\nu^{-1}$  ( $\nu$ : kinematic viscosity). The flow is inside a cubic box of side length  $L$ , having a cyclic boundary condition, so that the velocity field is made of discrete modes with the wavenumbers shaping a cubic lattice with the interval  $\Delta k = \frac{1}{2}$  (i.e.,  $L = 4\pi$ ). The total number of lattice points considered is  $32^3$ , but with the use of the alias-free transform method.<sup>6</sup> Our calculation was executed at  $R_0 = 50$  (i.e.,  $R_\lambda = 57.7$  as the Reynolds number referred to Taylor's microscale). The other difference between Orszag *et al.*'s calculation and ours is that we used the solenoidal representation of the Navier-Stokes equation<sup>7</sup> as well as the Runge-Kutta method for time integration.

Since type (1) of the initial energy spectrum is common to the aforementioned two works,<sup>4,5</sup> we can compare the results of energy decay using three different methods. If we adopt Tatsumi *et al.*'s definition as a standard scaling, where the initial energy spectrum is expressed as  $E_0(k/k_0)^4 \exp[-(k/k_0)^2]$ , the nondimensional time as  $E_0^{1/2} k_0^{3/2} t$ , and the Reynolds number  $R$  as  $E_0^{1/2} / \nu k_0^{1/2}$ , we have only to insert the new curves into one of their figures (see Fig. 1). Note here that the original Reynolds numbers in the work of McComb *et al.* ( $R_\lambda = 35$ ) and in ours must be changed to  $R = 38$  and  $R = 61$ , respectively.

The most interesting point is that the curves for these two  $R$ 's appear to be natural extensions from those by Tatsumi *et al.* for lower  $R$ 's, while they cross those by Tatsumi *et al.* for all  $R \geq 100$ . Since such a crossing of the energy decay curves hardly ever occurs for the case of Burgers' model turbulence,<sup>8</sup> it seems to be an unusual phenomenon. (If we look at the figure more carefully, we notice that all the curves for  $R \geq 100$  cross each other!) At present, it is not clear whether the phenomenon is peculiar to the modified zero fourth-order cumulant approximation theory or actually universal. This remains to be solved.

In this connection, it is useful to mention Herring's recent investigation,<sup>9</sup> which compares the results of the approaches by Edwards,<sup>10</sup> test-field model,<sup>11</sup> and Tatsumi *et al.* We may conclude from the figure there showing the energy decay of isotropic turbulence with an initial condition similar to (1) for  $R_\lambda = 600$ , that Tatsumi *et al.*'s approach gives too early an energy decay in comparison with the other two; while the power index of energy decay is predicted as

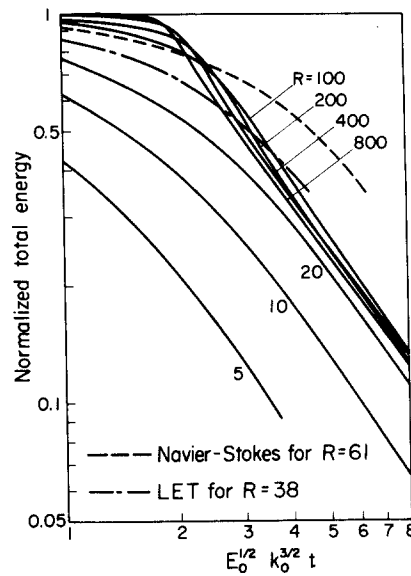


FIG. 1. The trend of energy decay of isotropic turbulence with the initial energy spectrum equivalent to Eq. (1).

about the same value by all three approaches. The latest energy decay is given by Edwards' approach. If we may conjecture extensively from our result of direct numerical simulation, the true curve of energy decay for such a high Reynolds number will fall in between the results by test-field model and Edwards, probably without any such crossing phenomenon as described above.

Finally, the inclusive work of Hogge and Meecham<sup>12</sup> on isotropic turbulence is worth noting. There, an energy-decaying turbulence which has started from almost the same initial condition as Herring<sup>9</sup> took is treated by the Wiener-Hermite expansion using a renormalized time-dependent base. While this method yields many plausible features of isotropic turbulence, such as the Kolmogorov inertial-range spectrum and the well-predicted Kolmogorov constant, the energy decay curve calculated at a high Reynolds number (1000 by their definition) is hardly comparable with any of the three curves in the above-mentioned figure by Herring.<sup>9</sup> As is easily known by transforming the original energy decay curve by Hogge and Meecham into a log-scale figure, the magnitude of the (log-)time-rate of (log-)energy decay is too small over the time interval considered (only about one initial-energy turn-over time) to find any generally acceptable power law of energy decay; though it may be expected to appear, only if the calculation proceeds much farther beyond this time interval.

## ACKNOWLEDGMENTS

This work was partially supported by the Scientific Research Fund of the Ministry of Education, Science, and Culture in Japan.

<sup>1</sup>For example, see K. Yamamoto and I. Hosokawa, *Phys. Fluids* **19**, 1423 (1976); J. Mizushima, *Phys. Fluids* **21**, 512 (1978); S. Kida, *Phys. Fluids* **24**, 604 (1981).

<sup>2</sup>R. H. Kraichnan, *Phys. Fluids* **7**, 1030 (1964).  
<sup>3</sup>S. A. Orszag and G. S. Patterson, Jr., *Phys. Rev. Lett.* **28**, 76 (1972); *Lect. Notes Phys.* **12**, 127 (1972).  
<sup>4</sup>T. Tatsumi, S. Kida, and J. Mizushima, *J. Fluid Mech.* **85**, 97 (1978); T. Tatsumi, in *Advances in Applied Mechanics*, edited by C-S. Yih (Academic, New York, 1980), pp. 39–130.  
<sup>5</sup>W. D. McComb and V. Shamugasundaram, *J. Fluid Mech.* **143**, 95 (1984).

<sup>6</sup>S. A. Orszag, *Stud. Appl. Math.* **50**, 293 (1971).  
<sup>7</sup>K. Yamamoto and I. Hosokawa, *J. Phys. Soc. Japan* **50**, 343 (1981).  
<sup>8</sup>I. Hosokawa and K. Yamamoto, *Phys. Fluids* **13**, 1683 (1970).  
<sup>9</sup>J. R. Herring, in *Frontiers in Fluid Mechanics*, edited by S. H. Davis and J. L. Lumley (Springer-Verlag, Berlin, 1985), pp. 68–87.  
<sup>10</sup>S. F. Edwards, *J. Fluid Mech.* **18**, 239 (1964).  
<sup>11</sup>R. H. Kraichnan, *J. Fluid Mech.* **47**, 513 (1971).  
<sup>12</sup>H. D. Hogge and W. C. Meecham, *J. Fluid Mech.* **85**, 325 (1978).

## Reduction of radial losses in a pure electron plasma

C. F. Driscoll, K. S. Fine, and J. H. Malmberg

*Department of Physics, University of California, San Diego, La Jolla, California 92093*

(Received 14 January 1986; accepted 11 March 1986)

A new pure electron-plasma containment apparatus exhibits radial losses approximately 20 times smaller than the prior apparatus. However, the new containment times show the same  $(L/B)^{-2}$  scaling with plasma column length and magnetic field as obtained previously. The radial transport is apparently induced by small irregularities that break the cylindrical symmetry of the magnetic and electric containment fields. The fact that the two devices show the same  $(L/B)^{-2}$  scaling suggests the dominance of a single generic process, although this process has not yet been identified.

A number of plasma physics and atomic physics experiments are based on confinement of unneutralized electrons or ions in cylindrically symmetric traps.<sup>1–6</sup> For the experiments reported here, a cylindrical column of electrons is confined by an axial magnetic field, and by negative potentials applied to electrodes at the ends of the column. Since the axial confinement is energetically assured, the plasma is lost only by radial transport across the magnetic field. This radial transport is constrained by conservation of the total canonical angular momentum of the particles and fields; the plasma can expand radially only if this angular momentum is changed as a result of external torques acting on the plasma.<sup>7</sup> Electron-neutral collisions can provide a torque and produce plasma expansion, with a rate proportional to the neutral pressure.<sup>8,9</sup> However, for the present experiments, the pressure is sufficiently low that electron-neutral collisions do not significantly contribute to the transport.

Rather, we observe plasma expansion as a result of an “anomalous” transport process that is independent of pressure. This transport is probably caused by small azimuthal asymmetries in the applied magnetic or electric fields. Experiments on a prior apparatus established that the anomalous transport rate depends strongly on the length  $L$  of the plasma column, as well as on the magnetic field  $B$ . With the magnetic field of the apparatus aligned for maximum cylindrical symmetry, the transport rates were observed to scale as  $(L/B)^2$  over more than five decades.<sup>1</sup>

A new apparatus has been constructed, with particular attention given to minimization of construction asymmetries in the electric and magnetic field structures. The magnetic solenoid was wound more accurately, the use of permeable materials was minimized, and the cylindrical containment electrodes were fabricated and aligned to closer tolerances. We find that the anomalous transport rates on the new apparatus show the same  $(L/B)^2$  scaling, but with a

rate coefficient 20 times smaller. This suggests the dominance of a single transport mechanism in both apparatuses, although this process has not yet been identified. Since all containment devices will have asymmetries, we believe this transport will be generic to all non-neutral-plasma experiments in this geometry. Further, it may have relevance to asymmetry-induced ion transport in neutral devices such as tandem mirrors.<sup>10–12</sup>

The cylindrical containment electrodes for the new apparatus are shown schematically in Fig. 1. There are eight electrically isolated cylinders of radius  $R_c = 3.81$  cm; all have length 7.62 cm except for L2, which is 3.81 cm long. One cylinder has four electrically isolated wall sections that can be used to launch and detect waves, but which are connected to a ground for these experiments. The containment electrodes are in a uniform static magnetic field that is varied over the range  $33 \leq B \leq 375$  G. The containment region is evacuated to an operating pressure  $P \leq 10^{-10}$  Torr.

The system is normally operated in an inject, hold, dump/measure cycle. Electrons emitted from a tungsten filament and grid assembly are trapped within the grounded cylinders between a dump gate (e.g., G2) and an injection gate (e.g., G1) by sequenced application of negative voltages to the dump and injection gates. The length of the trapped plasma column can be varied over the range  $4 \leq L \leq 40$  cm, determined by the cylinders chosen for confinement and by the voltages applied.

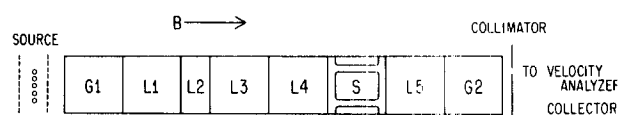


FIG. 1. The cylindrical containment electrodes.